Available online at www.sciencedirect.com
SCIENCE DIRECT®
Physica D 188 (2004) 292–313
PHYSICA D
www.elsevier.com/locate/physd

A mathematical model of motorneuron dynamics in the heartbeat of the leech

Pietro-Luciano Buono [a], A. Palacios [b,*]

[a] *Centre de Recherches Mathématiques, Université de Montréal, Montréal, Que., Canada H3C 3J7*
[b] *Department of Mathematics and Statistics, San Diego State University, Nonlinear Dynamics Group, San Diego, CA 92182-7720, USA*

Received 21 October 2002; received in revised form 24 July 2003; accepted 27 August 2003
Communicated by C.K.R.T. Jones

Abstract

The heartbeat of the medicinal leech is driven by direct contact between two arrays of motorneurons and two lateral blood vessels. At any given time, motorneurons exhibit one of two alternating states so that, on one side of the animal, the heart beats in a rear-to-front fashion (peristaltic), while on the other side the heart beats synchronously. Every 20 heartbeats, approximately, the two sides switch modes. It is known that the heartbeat rhythm is generated through burst of oscillatory activity produced by a central pattern generator (CPG) network of neurons. However, to the best of our knowledge, how the CPG activity is translated into peristaltic and synchronous rhythms in the motorneurons is yet unknown. In this work, we use symmetric systems of differential equations, accompanied with computational simulations, to investigate possible mechanisms for generating the motorneuron activity that characterizes the heartbeat of leeches and in particular the switching scenario.

PACS: 05.45.−a

Keywords: Coupled cell systems; Symmetry; Bifurcation

1. Introduction

Central pattern generators (CPGs) are networks of neurons, located in the central nervous system (CNS), whose function is to generate the rhythmic activity for various physiological functions such as locomotion, mastication and respiration [8,22]. To initiate a particular function, first the CNS translates the CPG rhythm into a coordinated pattern of activity and then, it sends it to motorneurons innervating muscle fibers. In many cases, the coordinated pattern is just a faithful image of the CPG rhythm. For instance, in many invertebrates and primitive vertebrates [14], it has been established that the fictive locomotion produced by the CPG and the actual rhythmic motor output are similar. This fact is often used as a modeling assumption for constructing realistic mathematical models for locomotor

* Corresponding author. Tel.: +1-619-5946808;
fax: +1-619-5946746.
E-mail address: palacios@euler.sdsu.edu (A. Palacios).

0167-2789/$ – see front matter © 2003 Elsevier B.V. All rights reserved.
doi:10.1016/j.physd.2003.08.003

CPG [1]. Many of these models, in turn, have already provided useful insight into the biological mechanisms for generating vertebrate locomotion [8]. Of particular interest to this work is the rhythmic activity of the heartbeat of the medicinal leech, which is also generated and controlled by a CPG [7]. In this case, however, the activity of the CPG does not translate, in a simple way, directly into the activity of the motorneurons that excite the muscles of the blood vessels to produce the heartbeat rhythm [28–30]. Instead, the motorneurons exhibit two alternating patterns of oscillations called synchronous and peristaltic. In the synchronous pattern, all motorneurons oscillate in phase with each other, while in the peristaltic state a rear-to-front wave of rhythmic activity propagates among the motorneurons. While on one side the motorneurons support a synchronous pattern, the motorneurons on the other side fire in a peristaltic pattern and after about 20 cycles the motorneuron networks on each side switch activity to the other pattern.

An important problem for theoretical and experimental biologists is to elucidate the properties that determine the behavior of any given network of neurons [15]. These properties normally include: intrinsic dynamics of neurons, network connectivity (i.e., which neurons communicate with each other), type of coupling between connected neurons, and network dynamics [15]. In the particular case of the leech's heartbeat, properties of the CPG have been studied for many years, see [5–7,12,19,23,25]. However, there have been only a few attempts [10,28–30] at understanding the properties of the motorneuron network and the interplay with the CPG dynamics. Golubitsky and Stewart [10] address the problem of describing the motorneuron dynamics through a network of coupled cells with $\mathbf{Z}_2$-symmetry, and with an architecture that resembles the CPG-motorneurons network. By introducing the concept of "interior symmetries", they are able to reproduce simultaneously (for the left and right subnetworks) synchronous and peristaltic states as a unique periodic solution, called synchro-traveling, of the entire coupled cell system. The problem of describing the periodic switching between synchro-traveling states, however, has not been addressed yet.

In this paper, we also study the synchronous and peristaltic oscillations that characterize the dynamics of the motorneurons that drive the heartbeat of the leech. However, we now propose an alternative approach to describe not only synchronous and peristaltic states but also the periodic switching problem. Since synchronous and peristaltic rhythms are common in systems of symmetrically coupled cells with symmetry group containing cyclic groups [2,11,13], our approach is based on approximating the network of motorneurons by a coupled system of n cells with $\mathbf{D}_n$-symmetry. We then consider the output from the CPG network as a forcing term acting on the motorneuron network. The main contributions of our approach are model independent and they can be summarized as follows. We assume that both oscillation patterns, synchronous and peristaltic, can be created via bifurcations of periodic solutions that occur in the neighborhood of a Hopf/Hopf bifurcation in the coupled cell system or network with $\mathbf{D}_n$-symmetry. Under this assumption, each branch of periodic solution has its own natural frequency of oscillation, independent of the frequency of other branches. Using numerical simulations, we then show the dependency of the frequency of synchronous and peristaltic oscillations on the driving frequency of the CPG. More specifically, we show how the output from the CPG can lead to frequency entrainment between synchronous and peristaltic oscillations, which is consistent with experimental results. Finally, we also propose a mechanism through which the inhibitory input from the CPG can induce periodic transitions between synchronous and peristaltic oscillations.

The paper is structured as follows. In Section 2 we present a detailed review of the structure and dynamics of the leech's heartbeat CPG and the oscillation patterns in the motorneurons. In Section 3 we explain the modeling assumptions that lead us to consider arrays of coupled motorneurons with $\mathbf{D}_n$-symmetry. We model these arrays by systems of coupled identical cells and explain the assumption that both states, synchronous and peristaltic, can arise via Hopf/Hopf mode interaction from a trivial solution. To be more precise, the synchronous state via a standard Hopf bifurcation and the peristaltic state via a symmetry-breaking Hopf bifurcation. In Section 4 we derive a system of differential equations, in normal form, consistent with the $\mathbf{D}_n$-symmetry of the network. We use the normal forms to study Hopf/Hopf mode interactions. More importantly, we argue that the frequency of synchronous and

peristaltic oscillations can be entrained with the frequency of the periodic forcing output from the CPG. We then present numerical simulations showing the in-phase and peristaltic states oscillating at the driving frequency of the CPG. In Section 6, we illustrate how the CPG output can force the oscillators to switch activity between two periodic solutions—one representing the synchronous state and one representing the peristaltic state. We conclude with a discussion where we compare our work with other modeling approaches.

2. Background on motorneuron and CPG dynamics

The heartbeat of the medicinal leech is composed of contractive rhythms executed by two muscular lateral blood vessels, which together with ventral and dorsal vessels form the circulatory system of the animal [7]. The rhythms of the blood vessels is driven by bursting activity from pairs of lateral *heart motorneurons* located in ganglia 3–18. Motorneurons on one side burst either with a synchronous pattern or a peristaltic pattern [7,12,19]. In the former case, all motorneurons burst in phase, and consequently, all blood vessels constrict simultaneously on all their length. In the latter case, the burst is in a rear-to-front fashion, thus producing a traveling wave of contracting blood vessels. These two types of myogenic rhythms are coordinated so that, while one side beats synchronously, the other beats peristaltically. Every 20 heartbeats, approximately, the two sides switch coordination states. Moreover, both types of oscillating patterns have the same frequency (Calabrese, personal communication).

Experiments conducted by Calabrese and collaborators [23,25] reveal that motorneurons behave as identical oscillators. Each oscillator fires tonically when it is isolated. Bursting activity in the motorneurons is then induced and controlled by cyclic inhibitory signals produced by a heartbeat CPG. The CPG consists of seven identified pairs of heart interneurons located in the first seven segmental ganglia, see Fig. 1.

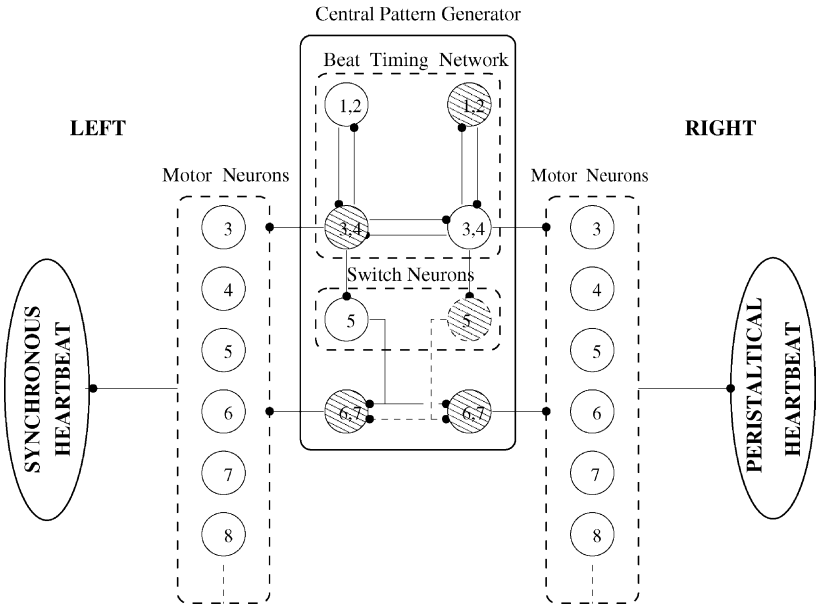

Fig. 1. Schematic diagram of networks of motorneurons and heart interneurons that generate the heartbeat of leeches. Motorneurons drive the heart rhythm by direct contact with blood vessels. In turn, the activity of the motorneurons is controlled, via inhibitory synapses (filled circles) by a CPG formed by heart interneurons. Shaded neurons fire synchronously with one another and out-of-phase with those not shaded.

Following the notation in [7], we denote by HN(i) a heart interneuron in ganglia i. Similarly, HE(i) denotes a motorneuron in ganglia i. The first four pairs of interneurons form a subnetwork, called the *beat timing network*. The two pairs of cells from the third and fourth ganglia, HN(3) and HN(4), drive the activity of this subnetwork. Each pair is connected to each other by reciprocal inhibitory synapses which allow them to produce alternating bursts of activity [6,7]. The other interneurons of the first and second ganglia act as coupling fibers connecting HN(3) and HN(4). The function of the timing network is to reset and entrain the rhythm of the entire CPG as follows. First, the timing network induces cells in the fifth ganglion into a high-frequency burst by interrupting their tonic action potential with inhibitory postsynaptic bursting input from cells HN(3) and HN(4). At any given time, only one of the HN(5) cells is active, while the other remains almost silent. Then, the active cell transfers, via inhibitory synapses, the activity of its ipsilateral side of HN(3) and HN(4) to both interneurons of the sixth and seventh ganglia. As a consequence, interneurons HN(6) and HN(7) oscillate in synchrony with each other, and with those cells HN(3) and HN(4) that are ipsilateral to the active HN(5) cell. Furthermore, all cells oscillate with the same wave form and with the same phase.

A critical experimental observation is the fact that the side of the body ipsilateral to the inactive HN(5) cell exhibits the peristaltic bursting mode, while the side ipsilateral to the active HN(5) interneuron shows the synchronous mode. When HN(5) switches activity state, the motorneurons switch their dynamics, see Fig. 2. For this reason, the HN(5) cells have been called *switching interneurons* and have been attributed the function of controlling the two coordination states. Now, since cells HN(3), HN(4), HN(6) and HN(7) are directly connected with the motorneurons, their activity generates the rhythmic activity seen in the motorneurons. Thus, when the activity of cells HN(3) and HN(4) is synchronized with that of cells HN(6) and HN(7), its ipsilateral side displays the synchronous mode, while when they are out-of-phase the ipsilateral side exhibits the peristaltic mode. Consequently, a fundamental problem is to understand how synchronous and out-of-phase rhythms in the CPG are translated into synchronous and peristaltic activity in the motorneuron network.

We now focus our attention on the interaction between interneurons in the CPG and motorneurons. Although the work by Thompson and Stent [28–30] and personal communication with Calabrese indicates that motorneurons

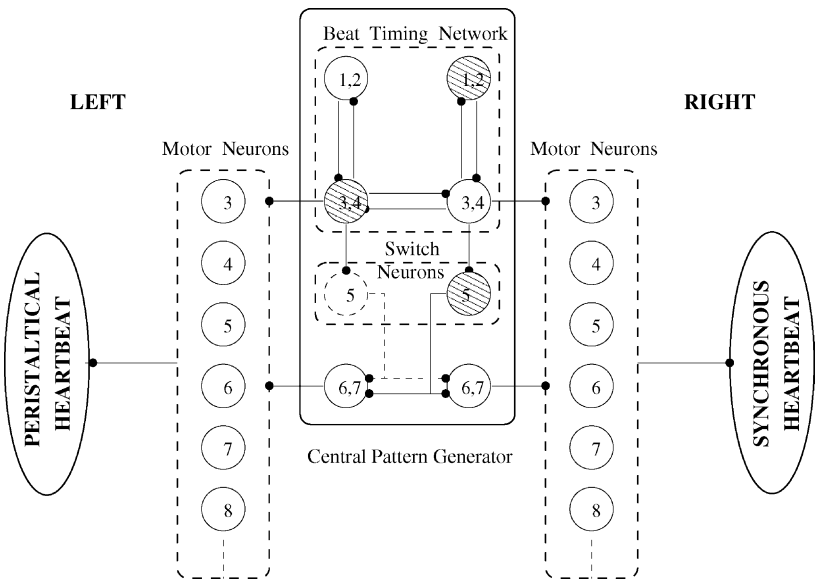

Fig. 2. Switching of activity by interneuron HN(5) induces a change of heart coordination state on each side of the leech.

are not directly connected to one another, it is possible that they might communicate through the axons that carry the inhibitory input from heart interneurons. Evidence of this type of communication is explained in the following section. Even if our type of network does not reflect exactly the anatomical connections in the body of the leech, we aim this work at gaining useful insight in the analysis of motorneuron switching patterns.

3. Modeling assumptions for network equations

The experimental works of Thompson and Stent [28–30] and Calabrese and coworkers [12] reveal a complex set of connections between heart interneurons and motorneurons as is shown in Fig. 3. Although the diagram shows no synaptic connections between motorneurons, it is possible for motorneurons to communicate via *antidromic* signals, or rectifying signals as they are described in the same work by Thompson and Stent. Next we explain this biological issue in more detail. Early work in theoretical and computational neuroscience assumed that action potential initiation in neurons of the CNS occurs primarily in the axon initial segment adjacent to the cell body (soma); that such action potential travels only along output axons; that dendrites behaved as passive cables; and that only dendrites and cell bodies could act as receptive areas for synaptic inputs [18]. Over the years, however, many experimental studies have shown that neural cells are far more complicated and, as a result, some of these assumptions had to be re-examined. For instance, it is now known that many dendrites of pyramidal cells are electrically active with voltage-dependent membrane conductances [17]. More importantly, experiments in neocortical pyramidal neurons have revealed that action potentials can also propagate backwards into the dendritic tree [26,27]. Furthermore, backward propagation has shown to be critical in explaining synaptic plasticity in Hebbian learning [20,21]. Since then, forward propagation of action potentials has been referred to as *orthodromic potentials*, and backward propagation as *antidromic potentials* or *antidromic spike invasion*.

In principle, it is then possible that the axons that carry the inhibitory inputs from heart interneurons to motorneurons also carry antidromic signals from one motorneuron to a neighboring one. Evidence of this type of connections in the mastication system of rabbits can be found in the work of Westberg et al. [32].

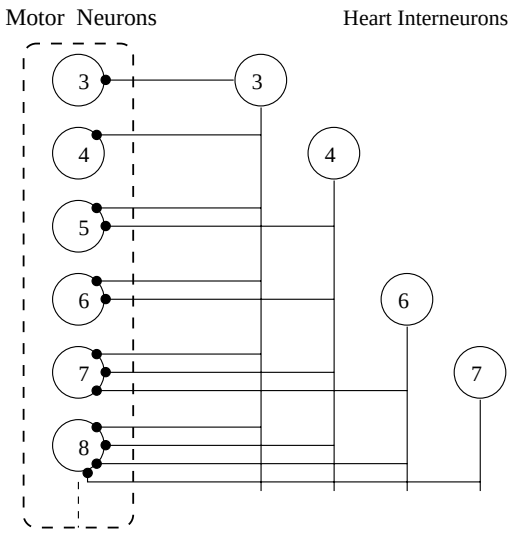

Fig. 3. Pattern of connections between heart interneurons and motorneurons for each side of the body of the leech.

In view of a first attempt to investigate the interaction between CPG and motorneurons, we adopt the simplifying assumption that motorneurons form linear arrays with synaptic connections among nearest neighbors. Since motorneurons behave as identical oscillators, it is then reasonable that we model each array on each side of the body by systems of coupled identical cells. We restrict the modeling of the CPG and motorneurons to one side of the network since the network is bilaterally symmetric and the activity of the CPG is periodic with one side of the CPG network half a period out-of-phase with the other side. In particular, the activity of HN(5) on the left is half a period out-of-phase with HN(5) on the right.

Epstein and Golubitsky [9] observed that the steady-states and periodic solutions in linear arrays can be studied by embedding the linear array into a circular array with twice the number of cells and with dihedral symmetry. Thus, we consider arrays of n motorneurons with dihedral $\mathbf{D}_n$-symmetry. We then model an interconnected network of n motorneurons by a coupled system of $\mathbf{D}_n$-symmetric differential equations of the form

$$\frac{\mathrm{d}X_i}{\mathrm{d}t} = f(X_i, \nu, \mu) + \sum_{j\to i} \alpha_{ij} h(X_i, X_j), \tag{1}$$

where $X_i = (x_{i1}, \ldots, x_{ik}) \in \mathbf{R}^k$ denotes the state variables of cell i, f is smooth and independent of i (since the cells are assumed to be identical), $\nu = (\nu_1, \nu_2)$ are the principal bifurcation parameters and $\mu = (\mu_1, \ldots, \mu_p)$ is a vector of parameters for the internal dynamics of each cell, h the coupling function between two cells, and α_{ij} a matrix of coupling strengths. We write the network equations in a more compact form

$$\frac{\mathrm{d}X}{\mathrm{d}t} = F(X, \nu, \mu, \alpha), \tag{2}$$

where $F : \mathbf{R}^N \to \mathbf{R}^N$, $X = (X_1(t), X_2(t), \ldots, X_n(t))$. Note that $N = kn$ for a network of n cells with k state variables in each cell. In the X variable, the synchronous mode corresponds to a periodic solution of (2) of the form

$$X_{\mathrm{s}}(t) = (X_1(t), X_1(t), \ldots, X_1(t)),$$

so that all n cells fire in phase and with the same wave form. Similarly, we can write the peristaltic state as a periodic solution of the form

$$X_{\mathrm{p}}(t) = (X_1(t), X_1(t-\phi), X_1(t-2\phi), \ldots, X_1(t-(n-1)\phi)),$$

in which consecutive cells now fire out-of-phase by a constant amount ϕ, though the wave form is the same. In general, periodic solutions exhibit either purely spatial symmetries, which fix a solution at any time, or spatio-temporal symmetries, which fix a solution after a phase shift. In the synchronous mode, all symmetries are purely spatial. Since any element of $\mathbf{D}_n$ leaves X_{s} unchanged, then $\mathbf{D}_n$ is the underlying group of spatial symmetries of X_{s}. In contrast, in the peristaltic mode any cyclic permutation of the cells must be coupled with an equal phase shift in time to leave X_{p} unchanged. We then identify $\tilde{\mathbf{Z}}_n$, the group of cyclic rotations of the plane through $0, \phi, \ldots, (n-1)\phi$, coupled with temporal shifts by the same amount, as the underlying group of spatio-temporal symmetries of X_{p}.

We assume that both patterns arise, via Hopf bifurcations, when a trivial solution $X = 0$ with $\mathbf{D}_n$-symmetry loses stability at $(\nu_1, \nu_2) = (0, 0)$. This implies that $(d_x F)_{000}$ has two pairs of complex eigenvalues crossing the imaginary axis with nonzero speed—one pair for each mode. Under the presence of $\mathbf{D}_n$-symmetry, these eigenvalues are either simple (standard Hopf bifurcation) or double (symmetry-breaking Hopf bifurcation). In the synchronous mode, we expect the eigenvalues to be simple since there is no change of symmetry in the bifurcating branch. In the peristaltic mode, however, we expect the eigenvalues to be double due to a symmetry-breaking bifurcation from the $\mathbf{D}_n$-symmetric trivial solution to the $\tilde{\mathbf{Z}}_n$-symmetric peristaltic state. Since the pairs of imaginary eigenvalues,

$\pm\omega_1\mathrm{i}$, for the standard Hopf, and $\pm\omega_2\mathrm{i}$, for the symmetry-breaking Hopf, have eigenspaces with different group actions, a necessary condition for a Hopf/Hopf mode interaction of this type is that the dimension of the cells must be at least 2.

Thus, at the codimension two point $(\nu_1, \nu_2) = 0$ we have a mode interaction between two branches of periodic solutions—one with synchronous oscillations and one with peristaltic oscillations. The parameters (ν_1, ν_2) are then called the unfolding parameters of the mode interaction in the network equations. In the following section we discuss this mode interaction in $\mathbf{D}_n$-symmetric systems of differential equations in normal form.

4. Mode interaction in normal forms

Under the previous assumptions, $(d_x F)_{000}$ has eigenvalues $\pm\omega_1\mathrm{i}$, $\pm\omega_2\mathrm{i}$ and $\pm\omega_2\mathrm{i}$, where ω_1 and ω_2 are the frequencies of oscillations at the onset of the synchronous and peristaltic states, respectively. After performing a center manifold reduction on (2), we arrive at a truncated reduced system of ODEs

$$\frac{\mathrm{d}z}{\mathrm{d}t} = g(z, \lambda_1(\nu, \mu, \alpha), \lambda_2(\nu, \mu, \alpha)), \tag{3}$$

where $z = (z_0, z_1, z_2) \in \mathbf{C}^3$, (λ_1, λ_2) are now the unfolding parameters in the normal forms, and $g(0, \lambda_1, \lambda_2) = 0$. The eigenvalues of $(d_z g)_{0,0,0}$ are the critical eigenvalues of $(d_x F)_{0,0,0}$ on the imaginary axis. By an appropriate change of coordinates we can also assume that (3) is in Poincaré–Birkhoff normal form up to any finite order. This introduces an extra $\mathbf{S}^1$ symmetry in the bifurcation of each motor pattern, so that g is now $\mathbf{D}_n \times \mathbf{T}^2$-equivariant ($\mathbf{T}^2 = \mathbf{S}^1 \times \mathbf{S}^1$). We can then choose coordinates $z = (z_0, z_1, z_2)$ such that the $\mathbf{D}_n \times \mathbf{T}^2$-action on $\mathbf{C}^3$ takes the following form:

$$\begin{aligned} &\gamma(z_0, z_1, z_2) = (z_0, \mathrm{e}^{\gamma\mathrm{i}} z_1, \mathrm{e}^{-\gamma\mathrm{i}} z_2), \qquad \kappa(z_0, z_1, z_2) = (z_0, z_2, z_1), \\ &\theta(z_0, z_1, z_2) = (\mathrm{e}^{\theta_1\mathrm{i}} z_0, \mathrm{e}^{\theta_2\mathrm{i}} z_1, \mathrm{e}^{\theta_2\mathrm{i}} z_2), \end{aligned} \tag{4}$$

where $\gamma = 2\pi/n \in \mathbf{Z}_n$, κ is a fixed element in $\mathbf{D}_n \sim \mathbf{Z}_n$, and $(\theta_1, \theta_2) \in \mathbf{T}^2$ [13]. It follows that $\mathbf{D}_n \times \mathbf{T}^2$ acts trivially on $(z_0, 0, 0)$, so that the synchronous mode now corresponds to a periodic solution of (3) lying in the invariant subspace $(z_0, 0, 0)$. Similarly, and depending on the direction of the shift, we can identify the peristaltic state as a periodic solution in either subspace $(0, z_1, 0)$ or $(0, 0, z_2)$. Next we derive $\mathbf{D}_n$-invariant functions and $\mathbf{D}_n$-equivariant mappings.

4.1. $\mathbf{D}_n$-invariants and $\mathbf{D}_n$-equivariants

In this section, we calculate $\mathbf{D}_n$-invariant functions and $\mathbf{D}_n$-equivariant mappings. The results depend on the parity of n. Thus, we define

$$m = \begin{cases} n & \text{if } n \text{ is odd,} \\ \frac{1}{2}n & \text{if } n \text{ is even.} \end{cases}$$

Proposition 4.1. *Every real-valued $\mathbf{D}_n \times \mathbf{T}^2$-invariant germ is a function of ρ, N, P, S and T, where*

$$\begin{aligned} &\rho = |z_0|^2, \qquad N = |z_1|^2 + |z_2|^2, \qquad P = |z_1|^2 |z_2|^2, \\ &S = (z_1 \bar{z}_2)^m + (\bar{z}_1 z_2)^m, \qquad T = \mathrm{i}(|z_1|^2 - |z_2|^2)((z_1 \bar{z}_2)^m - (\bar{z}_1 z_2)^m). \end{aligned}$$

Proof. We derive the $\mathbf{D}_n \times \mathbf{T}^2$-invariants by starting with the $\mathbf{T}^2$-invariants. Since $\mathbf{T}^2$ acts on $\mathbf{C}^3$ by $\theta \cdot (z_0, z_1, z_2) = (e^{\theta_1 i} z_0, e^{\theta_2 i} z_1 e^{\theta_2 i} z_2)$ the complex-valued $\mathbf{T}^2$-invariants are generated by

$$\rho = |z_0|^2, \qquad u_1 = z_1\bar{z}_1, \qquad u_2 = z_2\bar{z}_2, \qquad v = z_1\bar{z}_2, \qquad \bar{v} \tag{5}$$

with the relation $u_1u_2 = v\bar{v}$. The next step would be to compute generators for the $\mathbf{D}_n$ invariants—first in the (ρ, u_1, u_2, v) space and eventually in the (z_0, z_1, z_2) space. Observe, however, that since $\mathbf{D}_n$ acts trivially on z_0, and by its standard action on (z_1, z_2), the generators for the $\mathbf{D}_n$ invariants are the same as in a problem of Hopf bifurcation with $\mathbf{D}_n$-symmetry. It follows from Golubitsky et al. [13] that N, P, S and T, together with ρ, constitute a complete set of generators for the $\mathbf{D}_n \times \mathbf{T}^2$-invariants. □

Proposition 4.2. *The $\mathbf{D}_n \times \mathbf{T}^2$-equivariant germs $f : \mathbf{C}^3 \to \mathbf{C}^3$ are generated over the $\mathbf{D}_n \times \mathbf{T}^2$-invariants by the following mappings*:

$$V^1 = (z_0, 0, 0), \qquad V^2 = (0, z_1, z_2), \qquad V^3 = (0, z_1^2\bar{z}_1, z_2^2\bar{z}_2),$$
$$V^4 = (0, \bar{z}_1^{m-1} z_2^m, z_1^m \bar{z}_2^{m-1}), \qquad V^5 = (0, z_1^{m+1}\bar{z}_2^m, \bar{z}_1^m z_2^{m+1}).$$

Proof. Let $g(z) = (g_0(z), g_1(z), g_2(z))$ be a $\mathbf{D}_n \times \mathbf{T}^2$-equivariant mapping $\mathbf{C}^3 \mapsto \mathbf{C}^3$, where $z = (z_0, z_1, z_2)$. Commutativity of g with κ implies that $g_2(z_0, z_1, z_2) = g_1(z_0, z_2, z_1)$. Next we determine the mappings $g_0, g_1 : \mathbf{C}^3 \mapsto \mathbf{C}$. The $\mathbf{T}^2$-equivariant maps have the form

$$g_0(z_0, z_1, z_2) = p(\rho, u, v)z_0, \qquad g_1(z_0, z_1, z_2) = q(\rho, u, v)z_1 + r(\rho, u, v)z_2,$$

where $\rho \in \mathbf{R}$, $u = (u_1, u_2) \in \mathbf{R}^2$, and $v \in \mathbf{C}$ are defined as in (5). Again, since $\mathbf{Z}_n$ acts trivially on z_0 it follows from Golubitsky et al. [13] that the $\mathbf{Z}_n \times \mathbf{T}^2$-equivariants for g_1 are given by four generators

$$z_1, \qquad z_1^2\bar{z}_1, \qquad \bar{z}_1^{m-1} z_2^m, \qquad z_1^{m+1}\bar{z}_2^m.$$

Finally, since commutativity of g with κ implies that $g_2(z_0, z_1, z_2) = g_1(z_0, z_2, z_1)$ we arrive at the $\mathbf{D}_n \times \mathbf{T}^2$ equivariant maps $V^1, \ldots, V^5$. □

4.2. Branching equations

It follows from Propositions 4.1 and 4.2 that the general $\mathbf{D}_n \times \mathbf{T}^2$-equivariant mapping $g(z, \lambda_1, \lambda_2) \in \mathbf{C} \times \mathbf{C}^2$ has the form

$$g = A\begin{bmatrix} z_0 \\ 0 \\ 0 \end{bmatrix} + B\begin{bmatrix} 0 \\ z_1 \\ z_2 \end{bmatrix} + C\begin{bmatrix} 0 \\ z_1^2\bar{z}_1 \\ z_2^2\bar{z}_2 \end{bmatrix} + D\begin{bmatrix} 0 \\ \bar{z}_1^{m-1} z_2^m \\ z_1^m \bar{z}_2^{m-1} \end{bmatrix} + E\begin{bmatrix} 0 \\ z_1^{m+1}\bar{z}_2^m \\ \bar{z}_1^m z_2^{m+1} \end{bmatrix}, \tag{6}$$

where A, B, C, D, and E are complex-valued $\mathbf{D}_n \times \mathbf{T}^2$-invariant functions depending on two parameters λ_1 and λ_2. Additionally, the eigenvalue structure of g leads to $A(0) = \omega_1 i$ and $B(0) = \omega_2 i$. Solving $g = 0$ and using polar coordinates $z_0 = r_0 e^{i\theta_0}$, $z_1 = r_1 e^{i\theta_1}$, and $z_2 = r_2 e^{i\theta_2}$, we find periodic solutions that bifurcate from the trivial solution $z = 0$ at the codimension two point $(\lambda_1, \lambda_2) = (0, 0)$. These solutions are listed in Table 1, where all coefficients are evaluated at zero, λ_1 is held fixed, and $a^1 = \mathrm{Re}\, A$, $b^1 = \mathrm{Re}\, B$, $c^1 = \mathrm{Re}\, C$, $d^1 = \mathrm{Re}\, D$, and $e^1 = \mathrm{Re}\, E$. Observe that symmetry forces the existence of two conjugate peristaltic states. One lies in the subspace $(0, z_1, 0)$ and one in $(0, 0, z_2)$. In physical space, the two peristaltic states correspond to the two possible directions of oscillations of the motorneurons, rear-to-front and front-to-rear. From the mathematical point of view, however,

Table 1
Branches of solutions for $\mathbf{D}_n$ Hopf/Hopf mode interaction

Solution	Isotropy subgroup	Orbit representative	Branching equations
Trivial	$\mathbf{D}_n \times \mathbf{T}^2$	$(0, 0, 0)$	$z = 0$
Synchronous mode	$\mathbf{D}_n \times \mathbf{S}^1$	$(r_0, 0, 0)$	$\lambda_1 = -\left(\frac{a^1_\rho}{a^1_{\lambda_1}}\right) r_0^2$
Peristaltic mode 1	$\tilde{\mathbf{Z}}_n \times \mathbf{S}^1$	$(0, r_1, 0)$	$\lambda_1 = -\left(\frac{b^1_N + c^1}{b^1_{\lambda_1}}\right) r_1^2$
Peristaltic mode 2	$\tilde{\mathbf{Z}}_n \times \mathbf{S}^1$	$(0, 0, r_2)$	$\lambda_1 = -\left(\frac{b^1_N + c^1}{b^1_{\lambda_1}}\right) r_2^2$

these two cases are equivalent. Thus, without loss of generality, in what follows we choose to work with the peristaltic state that lies in the invariant subspace $(0, 0, z_2)$.

4.3. Stability analysis

We now determine the stability properties of each motor pattern through the eigenvalues of $(d_z g)$. We do this by considering the isotypic decomposition of $\mathbf{C}^3$ into a direct sum of Σ-irreducible subspaces

$$\mathbf{C}^3 = V_0 \oplus V_1 \oplus V_2.$$

In Table 2, we show the isotypic decomposition by each of the isotropy subgroups of solutions. Note that $\mathrm{Fix}(\Sigma) = V_0$, for each subgroup Σ. Furthermore, observe that $(\mathbf{D}_n \times \mathbf{T}^2)/\Sigma$ forces one eigenvalue of dg to be zero. The corresponding null vector is also listed in Table 2. In each case, the stability of solutions with maximal isotropy is determined by $\mathrm{tr}(dg|V_j)$. We compute the Jacobian dg in complex coordinates

$$(dg)(\zeta) = g_{z_0}\zeta_0 + g_{\bar{z}_0}\bar{\zeta}_0 + g_{z_1}\zeta_1 + g_{\bar{z}_1}\bar{\zeta}_1 + g_{z_2}\zeta_2 + g_{\bar{z}_2}\bar{\zeta}_2,$$

where $\zeta = (\zeta_0, \zeta_1, \zeta_2)$, $g = (g^0, g^1, g^2)$ and $g_{z_j} = (g^0_{z_j}, g^1_{z_j}, g^2_{z_j})$. The sign of the eigenvalues of dg are also listed in Table 2.

Let σ_1 and σ_2 denote the eigenvalues of $(d_z g)|V_2$ along the synchronous and peristaltic branch, respectively. Using the branching equations from Table 1, we can write these eigenvalues in terms of λ_1. Direct calculations yield

$$\sigma_1 = \delta_1\lambda_1, \quad \delta_1 = b^1_{\lambda_1} - \frac{b^1_\rho a^1_{\lambda_1}}{a^1_\rho}, \qquad \sigma_2 = \delta_2\lambda_1, \quad \delta_2 = a^1_{\lambda_1} - \frac{a^1_N b^1_{\lambda_1}}{b^1_N + c^1}.$$

Table 2
Isotypic decomposition by isotropy subgroups of $\mathbf{D}_n \times \mathbf{T}^2$-symmetric normal forms

Solution	Isotypic component	Null vectors	Sign of eigenvalues
Synchronous mode	$V_0 = (z, 0, 0)$	(i, 0, 0)	V_0: $0, a^1_\rho$
	$V_1 = (0, z, 0)$		V_1: b^1 (twice)
	$V_2 = (0, 0, z)$		V_2: b^1 (twice)
Peristaltic mode	$V_0 = (0, 0, z)$	(0, 0, i)	V_0: $0, b^1_N + c^1$
	$V_1 = (0, z, 0)$		V_1: $-c^1$ (twice)
	$V_2 = (z, 0, 0)$		V_2: a^1 (twice)

It follows that the synchronous mode is asymptotically stable if $a^1_\rho < 0$ and $\sigma_1 < 0$. Similarly, the peristaltic mode is asymptotically stable when $b^1_N + c^1 < 0$, $c^1 > 0$, and $\sigma_2 < 0$. Each branch bifurcates supercritically ($\lambda_1 > 0$) if $a^1_{\lambda_1} > 0$ and $b^1_{\lambda_1} > 0$, respectively, and subcritically ($\lambda_1 < 0$) otherwise.

5. Transitions in motorneuron dynamics

The stability results of the previous section suggest two possible approaches that can lead to transitions between synchronous and peristaltic behavior. In the first approach, we assume that both branches of oscillatory solutions bifurcate supercritically and that all eigenvalues, except for σ_1 and σ_2, are negative. We also assume that the coefficients are such that $\mathrm{sgn}(\delta_1) = -\mathrm{sgn}(\delta_2)$. Then a periodic change in the signs of δ_1 and δ_2, while holding λ_1 fixed, would periodically change the stability properties of each branch. At any given time, the network would exhibit one periodic solution only, either X_s or X_p. But as time evolves the network would execute periodic excursions between these two solutions. From the biological point of view, changing δ_1 and δ_2 would probably require changing numerous parameters in the intrinsic dynamics of each neuron and in the network architecture. An alternative approach is the following.

Assume that $b^1_{\lambda_1} > 0$, $a^1_{\lambda_1} > 0$, and $\mathrm{sgn}(p^1_{\lambda_1}) = -\mathrm{sgn}(a^1_{\lambda_1})$, so that one branch bifurcates supercritically while the other bifurcates subcritically. If $\delta_1 > 0$ (<0) and $\delta_2 < 0$ (>0), then the peristaltic pattern bifurcates supercritically (subcritically) while the synchronous state bifurcates subcritically (supercritically). In contrast to the previous approach, observe that now both branches of solutions are simultaneously stable. Under these assumptions, it is now the bifurcation parameter λ_1 that needs to change periodically for the network dynamics to alternate periodically between the two motor patterns of solutions (Fig. 4).

5.1. Network properties

We now investigate the network properties that would have to be involved to realize the transition between synchronous and peristaltic oscillations as described in the second approach. We start by assuming the coupling function h to be linear (nonlinear coupling will be considered as well) so that the second term in (1) can be written in the form $L(\alpha)X$, where $X = (X_1(t), X_2(t), \ldots, X_n(t))$, $\alpha = (\alpha_{11}, \ldots, \alpha_{n1}, \ldots, \alpha_{1n}, \ldots, \alpha_{nn})$, and L is an $n \times k$ matrix that is defined by the coupling strengths α. Next we split the internal dynamics of each cell into its linear part (with respect to X and ν), $M(\mu)X$, and nonlinear part, $T(\nu)X + \hat{f}(X)$. Since the cells are identical, both M and T are block diagonal matrices. We can then write the network equations in the form

$$\frac{\mathrm{d}X}{\mathrm{d}t} = [M(\mu) + L(\alpha, \mu)]X + T(\nu)X + \hat{f}(X). \tag{7}$$

In this new form, it is easier to see that for some fixed values of α_{ij} and μ_k, the critical eigenvalues of $M + L$ are the critical eigenvalues of $(d_x F)_{000}$ on the imaginary axis (see Eq. (2)), which lead to a mode interaction between a standard Hopf bifurcation and a symmetry-breaking Hopf bifurcation at $X = 0$ and $(\nu_1, \nu_2) = (0, 0)$.

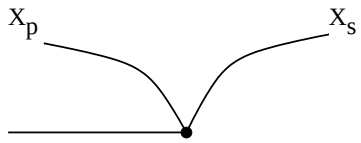

Fig. 4. Switching scenario: one branch bifurcates supercritically and one subcritically. A periodic change in the bifurcation parameter λ_1 would induce the network to switch periodically between solutions of each branch.

We assume that in order to obtain the appropriate conditions for the mode interaction described above, μ, ν, and some values of α_{ij}'s must be fixed at the bifurcation point. The remaining α_{ij}'s can be used as unfolding parameters so that $\lambda_1 = \lambda_1(\alpha_{ij})$, for some i, j. This suggests that changes in the coupling strength can be the source of changes in λ_1. For a nonlinear coupling function, the α_{ij}'s that are not fixed in its nonlinear part can be combined with the other α_{ij}'s. Together, all nonfixed α_{ij}'s can serve as unfolding parameters and λ_1 would remain a function that depends on coupling strengths. In practical terms, it is more likely that the CPG output can change the coupling strength as opposed to changing various auxiliary parameters. Consequently, we pursue this approach.

5.2. Frequency entrainment via CPG dynamics

In this section, we argue that the dynamics of the CPG plays a second role in addition to the previously discussed role of driving the motorneuron activity. More specifically, we argue that the CPG output acts also as a time periodic forcing, which causes the synchronous and peristaltic periodic solutions to oscillate at a common frequency, i.e., frequency entrainment.

Suppose that the parameters are such that the peristaltic mode is asymptotically stable. Consider the system of equations of the motorneurons dynamics as

$$\frac{\mathrm{d}X}{\mathrm{d}t} = F(X) + \epsilon p(t), \tag{8}$$

where X and f are as in Eq. (2), p is a time T-periodic map, and ϵ a parameter. One can show that in a neighborhood of a periodic solution, in this case the peristaltic pattern, the dynamics of the phase ϕ is given by the equation

$$\frac{\mathrm{d}\phi}{\mathrm{d}t} = \omega_0 + \epsilon Q(\phi, t),$$

where Q is a smooth T-periodic function of t, see for instance [24]. Thus, the phase space is a torus, $0 \leq \phi \leq 2\pi$, $0 \leq t \leq T$. By taking a section of the torus, we define a Poincaré mapping

$$\phi_{n+1} = \phi_n + \eta + \epsilon P(\phi_n), \tag{9}$$

where P is some smooth function. This map, which is also a circle map, describes the dynamics of ϕ on the torus phase space, where $\eta = \omega_0 T = 2\pi T/T_0$. It is well known that if $T \sim T_0$ and for ϵ large enough the circle map (9) lies in the 1:1 Arnold tongue. Thus the periodic solution and the periodic forcing are synchronized.

Hence, it is possible to entrain the synchronous and peristaltic solutions to oscillate at the same frequency as that of the forcing. In the next section, we show numerical simulations verifying this assertion.

6. Computer simulations

In this section, we consider the second switching scenario and discuss a method that would explain how the CPG output can be used to force the eigenvalue λ_1 to periodically change sign. We then carry out computer simulations with the normal form equations (6) and with a model of heart interneurons to demonstrate the results of the interaction between the CPG and the array of motorneurons. We finish this section with a description of a technique for visualizing the patterns of oscillations in the coupled cell system. The advantage of this technique is that it does not require computer simulations of the actual network equations.

6.1. A model for heart interneurons

We simulate the inhibitory input from the CPG through numerical simulations of a model for heart interneurons HN(3) and HN(4). The model, developed by Calabrese et al. [7,23], incorporates the escape mechanism of Wang and Rinzel [31] for generating alternating bursting activity. Each neuron is modeled as an isopotential compartment with Hodgkin and Huxley [16] intrinsic dynamics and synaptic conductances through

$$-C\frac{\mathrm{d}V}{\mathrm{d}t} = \left(\sum_{\text{ion}} I_{\text{ion}}\right) + I_{\text{L}} + I_{\text{SynG}} + I_{\text{SynS}} - I_{\text{Applied}}, \tag{10}$$

where I_{ion} represents a fast Na^+ current that mediates spikes, two low-threshold Ca^{2+} currents, three outward K^+ currents, a hyperpolarization activated inward current, and a low-threshold persistent Na^+ current, I_{L} the leak current, I_{SynG} a graded synaptic current, I_{SynS} the spike-mediated synaptic current from all presynaptic sources, and I_{Applied} the injected current. Computer simulations of this model, shown in Fig. 5, have been validated by experimental results.

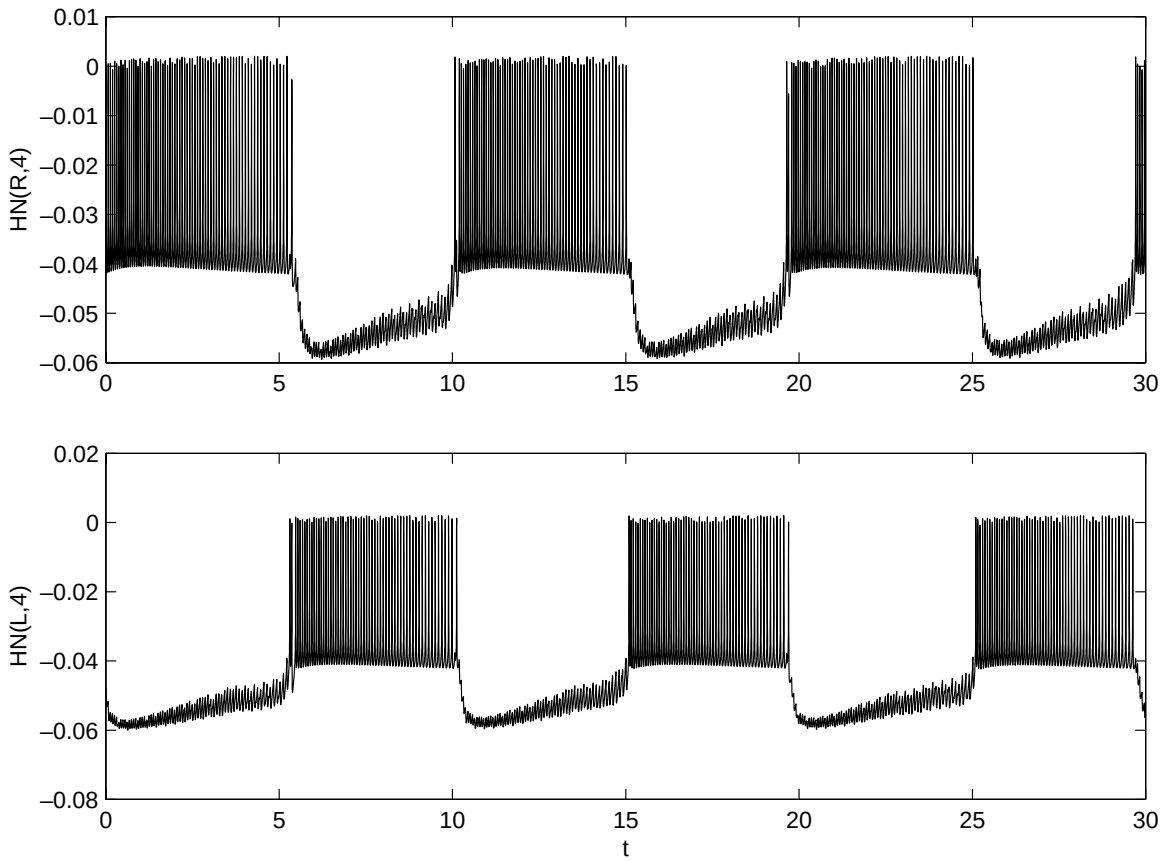

Fig. 5. Simulated rhythmic activity of two reciprocally inhibitory heart interneurons.

6.2. Blending of inhibitory input from CPG

Let $V_{\mathrm{HN}(i)}$ denote the voltage output of interneuron i, calculated according to Eq. (10). As we mentioned earlier, whether the heart beats synchronously or peristaltic depends mainly on whether the voltage output $V_{\mathrm{HN}(3)}$ and $V_{\mathrm{HN}(4)}$ is in-phase or out-of-phase with the voltage output $V_{\mathrm{HN}(6)}$ and $V_{\mathrm{HN}(7)}$, respectively. This conclusion leads us to conjecture the existence of a *switching function* for λ of the form

$$\lambda_1(V_{\mathrm{HN}(i)}) = \begin{cases} \lambda_1^+ > 0 & \text{if CPG output is in-phase,} \\ \lambda_1^- < 0 & \text{if CPG output is out-of-phase,} \end{cases}$$

where $i = 3, 4, 6, 7$. Considering the second switching scenario of Section 5, when $\lambda_1 = \lambda_1^+$ the motorneurons would tend to oscillate synchronously, while $\lambda_1 = \lambda_1^-$ would induce them to oscillate in a peristaltic wave. In the present work, we do not attempt to investigate the exact bio-mathematical expression of such switching function. We propose, however, a phenomenological expression that can provide insight into the role of the CPG output. We derive such an expression as follows. We first use the fact that the CPG output can be described as an in-phase/out-of-phase state that mimics an on/off state of a switch through the following voltage blending function:

$$V_{\mathrm{CPG}} = |V_{\mathrm{HN}(3)} + V_{\mathrm{HN}(4)} - V_{\mathrm{HN}(6)} - V_{\mathrm{HN}(7)}|, \tag{11}$$

where $V_{\mathrm{CPG}} = 0$ if the CPG output is in-phase, otherwise $V_{\mathrm{CPG}} = 2|V_{\mathrm{HN}(3)}|$ if it is out-of-phase. Observe that, according to the experimental description of the heartbeat, V_{CPG} would alternate periodically (approximately every 20 heartbeats) between these two values. Then a periodic switching between λ_1^+ and λ_1^- can be realized through a reverse sigmoid function of the form

$$\lambda_1(V_{\mathrm{CPG}}) = s_1 - \frac{s_2}{1 + \exp[(V_{\mathrm{CPG}} - V_{\mathrm{T}})/s_{\mathrm{T}}]}, \tag{12}$$

where V_{T} is a threshold value, s_1, s_2 and s_{T} are scaling parameters. In particular, $s_1 = \lambda_1^+$ and $s_1 - s_2 = \lambda_1^-$. Note that $\lambda_1 \to s_1$ if $V_{\mathrm{CPG}} \to \infty$, while $\lambda_1 \to s_1 - s_2$ if $V_{\mathrm{CPG}} \to -\infty$. In other words, the sigmoid shape of (12) accompanied with the periodic changes in V_{CPG}, would induce λ_1 to alternate periodically between λ_1^+ and λ_1^-.

6.3. Integration of normal form equations

Next we carry out computer simulations of the normal form equations (6), with λ_1 varying according to (12). For illustrative purposes, we consider a network of $n = 4$ motorneurons with $\mathbf{D}_4$ symmetry—the symmetry group of a square. In order to simulate the output from the CPG, we add a periodic perturbation to the normal forms through a term of the form $\epsilon(\sin(w_{\mathrm{d}}t) + \cos(w_{\mathrm{d}}t)\mathrm{i})$, where ω_{d} is the frequency of the driving force or perturbation. Then the actual equations that we integrate are shown below

$$\begin{aligned} &\dot{z}_0 = Az_0 + \epsilon(\sin(w_{\mathrm{d}}t) + \cos(w_{\mathrm{d}}t)\mathrm{i}), \qquad \dot{z}_1 = Bz_1 + Cz_1^2\bar{z}_1 + D\bar{z}_1z_2^2 + Ez_1^3\bar{z}_2^2, \\ &\dot{z}_2 = Bz_2 + Cz_2^2\bar{z}_2 + Dz_1^2\bar{z}_2 + E\bar{z}_1^2z_2^3 + \epsilon(\sin(w_{\mathrm{d}}t) + \cos(w_{\mathrm{d}}t)\mathrm{i}). \end{aligned} \tag{13}$$

Parameter values are: $\omega_{\mathrm{IP}} = 1.37$, which is the frequency of the in-phase solution, $\omega_{\mathrm{TW}} = 0.97$, which is the frequency of the traveling wave, and $\omega_{\mathrm{d}} = 8.0$, which is the frequency of the driving periodic force from the CPG. The main coefficients are defined below

$$\begin{aligned} &A = a^1 + a^2\mathrm{i}, \quad a^1 = 10\lambda - 4.0\rho + 2.9N, \ \ a^2 = \omega_{\mathrm{IP}}, \\ &B = b^1 + b^2\mathrm{i}, \quad b^1 = -10.0\lambda + 3.9\rho - 4N, \ \ b^2 = \omega_{\mathrm{TW}}, \qquad C = 1.0, \qquad D = 1.0, \qquad E = 1.0, \end{aligned}$$

and all other coefficients are set to zero. Results of the numerical integration of (13) with $\epsilon = 0$, i.e., the CPG output is only used for switching purposes, are shown in Fig. 6. Observe that, in agreement with the experimental work, the synchronous mode appears when the CPG output is in phase, while the peristaltic state appears when the CPG output is out-of-phase. Observe also that, in agreement with the normal form derivation and with the fact that $\epsilon = 0$, the frequencies of oscillations of these two states are not equal. Now we consider the second role of the CPG as a periodic forcing on the motorneuron dynamics and set $\epsilon > 0$. Upon gradually increasing the value of ϵ, the simulations reveal a threshold value, approximately $\epsilon = 7.0$, which marks the onset of frequency entrainment, see Figs. 7 and 8. We do not attempt to measure the size of this region but rather, we wish to interpret the results as a suggestion that the CPG output might be playing a double role in the heartbeat dynamics. In one role, it serves as a switching function between two modes of oscillations through periodic changes in λ_1, which can be associated with coupling strengths. In the other role, the CPG output can act as a periodic forcing that leads to frequency entrainment between in-phase and peristaltic oscillations.

6.4. Visualization of oscillations in network equations

In order to visualize the actual oscillations at the cell level of the motorneurons, further simulations of the cell system equations (2) would be needed. Performing these simulations, however, is more complicated than the normal form simulations because they require that we find, in the cell system, a center eigenspace of the same dimension as the normal forms. Additionally, we would also have to find parameter values of the cell system that match those of the normal form equations. One way of finding these parameter values is through a *center manifold* reduction from the ring of cells to the normal form equations. A term-by-term comparison of the reduced equations with the normal forms would then lead to the desired parameter values. For visualization purposes, however, it is possible to map the solutions of the normal forms to solutions of the cell system without performing the center manifold reduction. We now illustrate the ideas using previous normal form simulations from a network with $n = 4$ cells.

Recall first that the previous normal form simulations took place on $\mathbf{R}^6$. Then the $\mathbf{D}_n$-symmetric cell system must have a six-dimensional real center eigenspace with a Hopf/Hopf mode interaction, one standard and one symmetry-breaking. For the standard Hopf branch, the linearization of the network equations (2) must have a pair of complex eigenvalues with eigenspace invariant under the trivial action of $\mathbf{D}_n$. For the symmetry-breaking branch, we also need a pair of complex eigenvalues but with eigenspace invariant under the standard action of $\mathbf{D}_n$. We set the size of the cells to be $k = 2$, so that the ring of four cells is eight-dimensional. Next, we use the fact that the smooth mapping from a $\mathbf{D}_4$-symmetric cell system, with Hopf/Hopf (standard and symmetry-breaking) mode interaction, to the $\mathbf{D}_4 \times \mathbf{T}^2$-equivariant normal form is onto. This map is given by the composition of the center manifold reduction with the Poincaré–Birkhoff normal form transformations. Here we assume that all possible forms of cell coupling, linear and nonlinear, are allowed.

Let $z = (z_1(t), z_2(t), z_3(t))$ denote the simulations of the normal form equations (6). Define vectors $V_1(t) = z$ and $V_2(t)$ to be the solution of a system of ODEs of the form

$$\frac{\mathrm{d}V_2}{\mathrm{d}t} = -rI_2V_2,$$

where r is a real-valued scaling factor, and I_2 a 2×2 identity matrix. Observe that $V_1 \in \mathbf{R}^6$ and $V_2 \in \mathbf{R}^2$. Next, we embed the cycle in $\mathbf{R}^8$ by defining

$$V(t) = [V_1, V_2].$$

It follows that V_1 is asymptotically stable inside $\mathbf{R}^8$ and the flow restricted to the center eigenspace is exactly V_1. We then map V to a vector solution X of the coupled cell system (2) by applying the transformation $X = PQV$, where P

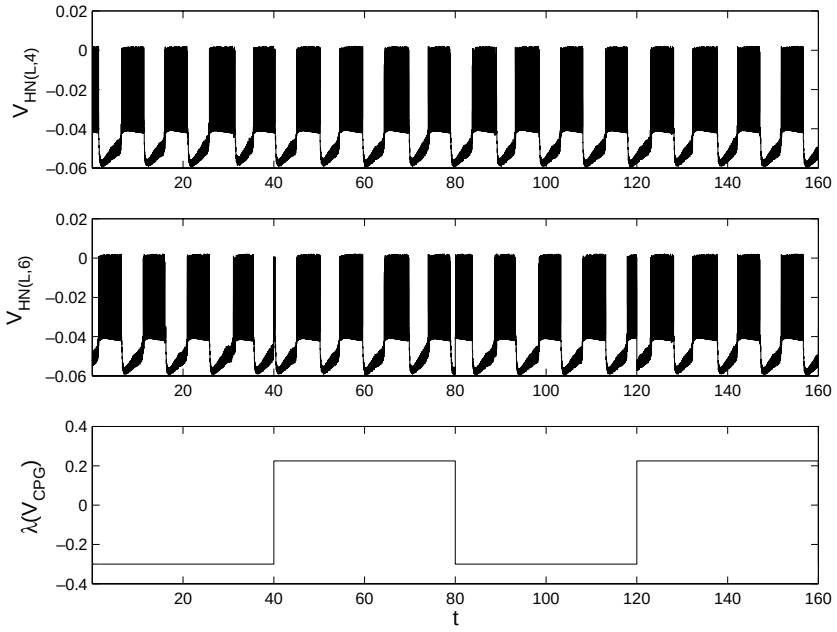

(a) CPG Input

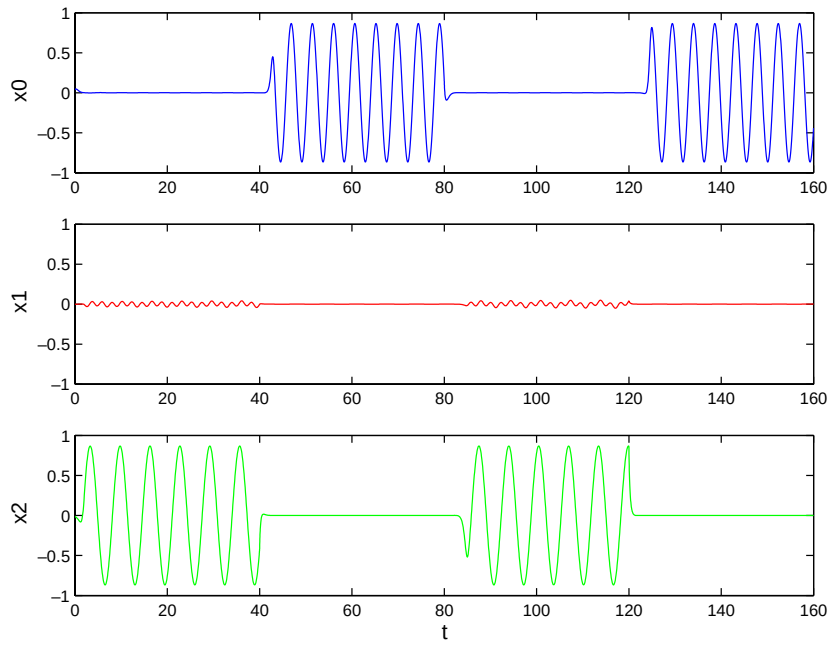

(b) Unperturbed Normal Form Output

Fig. 6. (a) Out-of-phase inhibitory rhythmic input from the CPG ($\lambda_1 < 0$) induces (b) peristaltic oscillations in the $(0, 0, x_2)$ subspace of the normal form simulations. On the contrary, when the input from the CPG is in-phase ($\lambda_1 > 0$), a switch to the synchronous mode $(x_0, 0, 0)$ occurs. Observe that the frequency of oscillation in each mode is different.

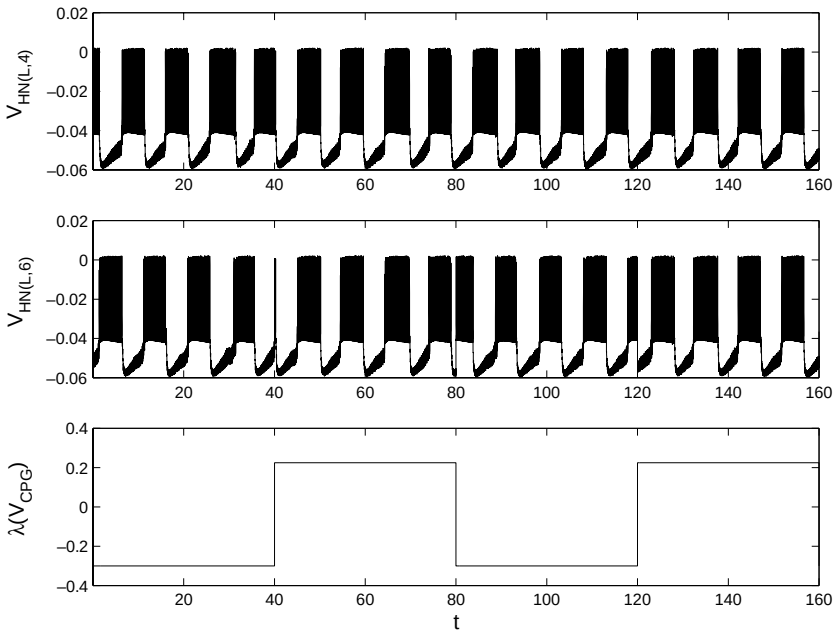

(a) CPG Input

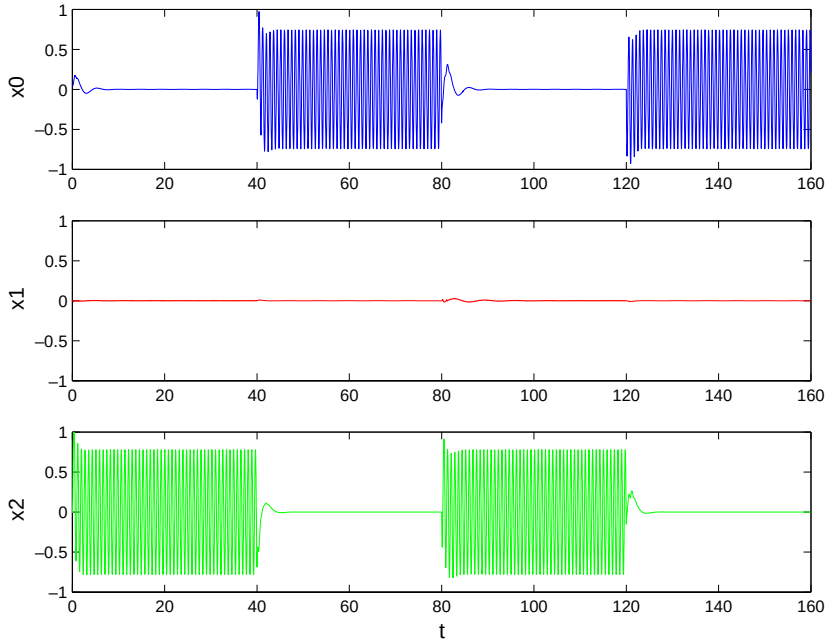

(b) Perturbed Normal Form Output

Fig. 7. Periodic perturbation of the normal forms can lead to frequency entrainment between peristaltic and in-phase oscillations in the simulations of Fig. 6.

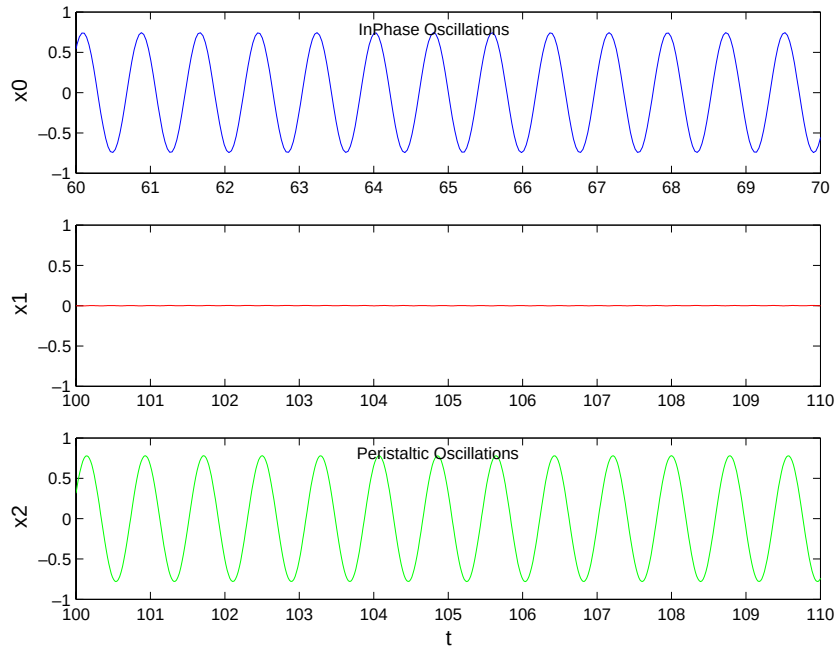

Fig. 8. Enlargement of peristaltic and in-phase oscillatory states of Fig. 7 further confirms the occurrence of frequency entrainment in the normal form simulations.

is a diagonalization matrix whose columns are the eigenvectors of the action of $\mathbf{D}_4$ on $\mathbf{C}^{3k}$, and Q defines a second linear transformation so that the $\mathbf{D}_4$-action on the center eigenspace of the cell system is the same as the action (4) on the normal forms. Before we apply the transformations, we need to break the $\mathbf{T}^2$-symmetry of the normal forms since $\mathbf{T}^2$ is not a symmetry of the coupled cell system. We do this using $\mathbf{D}_4$-equivariant terms. The choice of a $\mathbf{D}_4$-equivariant term is arbitrary—some choices are better than others. We now perform the transformation with $V(t)$ as defined above and with $r = 1$. The results are shown in Figs. 9 and 10, where a plot of the CPG input is included to aid the visualization of the switching times.

7. Discussion

The intricate dynamics of the motorneurons that produces the heartbeat of the leech is interesting in both its biological and mathematical aspects. In this paper, we have focused our attention on studying the biological aspects, through nonlinear dynamics techniques, for the generation of synchronous and peristaltic periodic states. In particular, we have provided a possible mathematical framework for producing synchronous and peristaltic states in a network model of motorneuron dynamics. More importantly, we have studied the role that the CPG plays in the switching mechanism and frequency entrainment of these periodic states, and have described a possible scenario for the CPG output to trigger a change of activity from one state to the other.

In our approach, we have tried to use as much biological information of the system under study. Some simplifying assumptions, however, have been made. For instance, we have assumed an approximate $\mathbf{D}_n$-symmetry in the motorneurons network. Also, we have made some underlying assumptions about connections between the motorneurons, and about the exact nature of in-phase and traveling wave patterns, even though the experimental

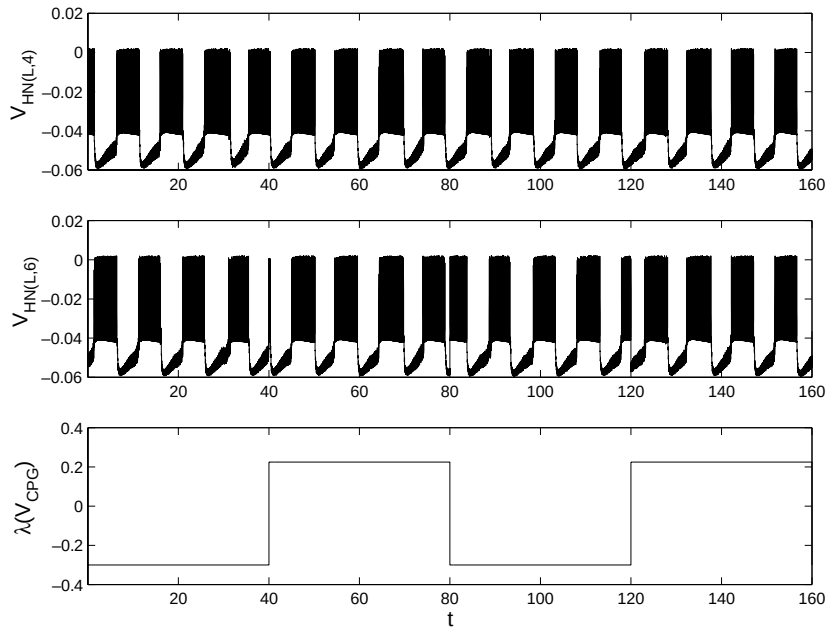

(a) CPG Input

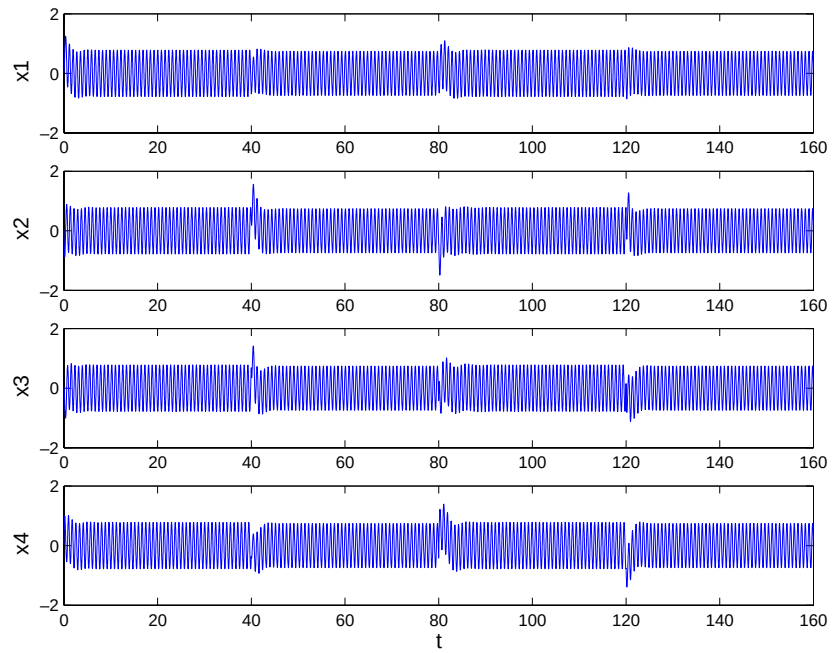

(b) Coupled Cell System Output

Fig. 9. Conversion of oscillatory behavior from the normal forms (see Fig. 7) into oscillations of the coupled cell system (2). Similar to the normal form simulations, when the CPG perturbations are in-phase, all cells oscillate synchronously. In contrast, when the perturbations are out-of-phase, the oscillations switch to the peristaltic mode.

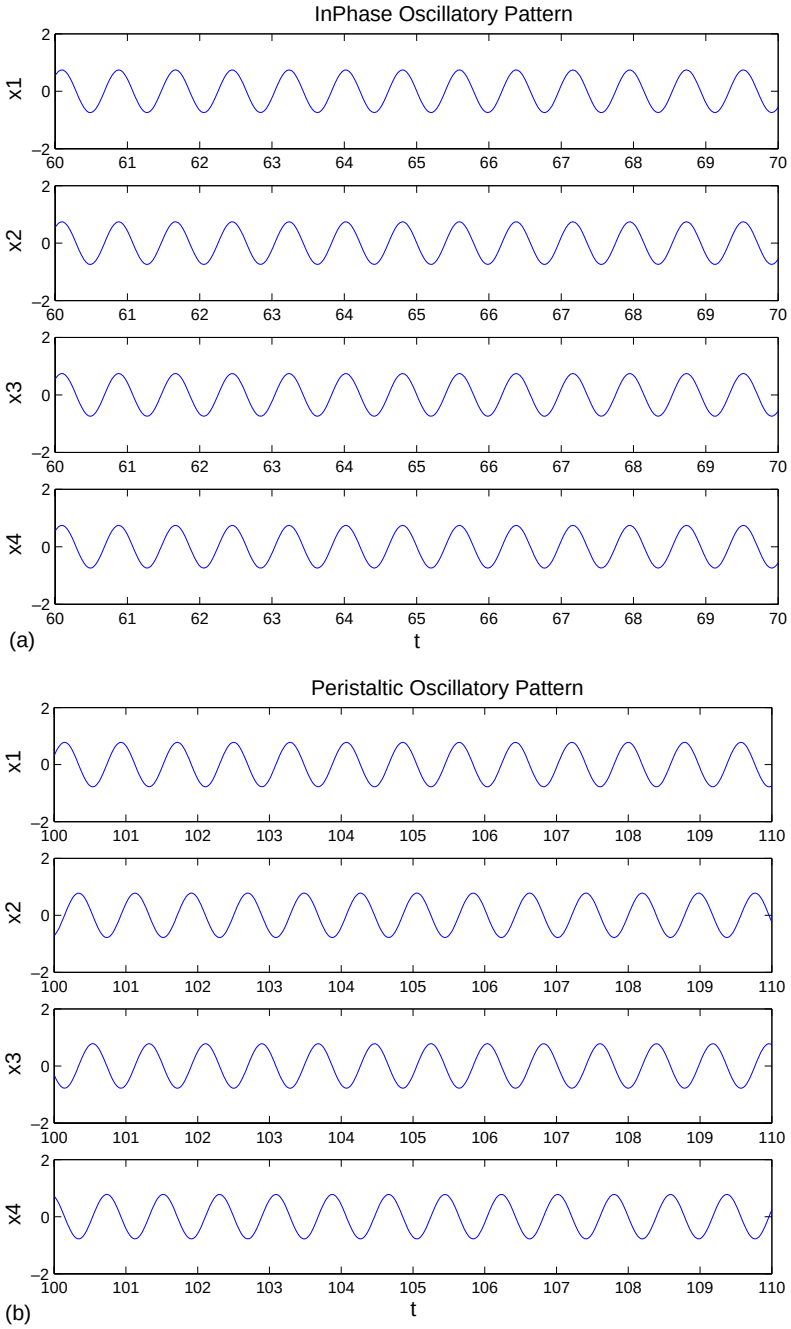

Fig. 10. Enlargement of (a) in-phase and (b) peristaltic oscillatory states of Fig. 9 further reveal frequency entrainment in simulations of (2).

measurements do not show exact peristaltic and synchronous periodic activity. That is, in the rear part of the network, the experimental peristaltic wave appears to be slower, while the synchronous wave shows also some deviations. Nevertheless, we believe that our underlying assumptions have sufficient advantages to justify their use. Mainly, they enable us to produce periodic states with dynamics close to the experimentally observed dynamics. Another point

of consideration to justify our approach is the well-documented fact that small symmetry-breaking perturbations from symmetric states retain approximate symmetries. This fact could explain the nonexact symmetries that are observed during experiments.

Preceding this work, another approach to study the motorneuron activity in leeches was proposed by Golubitsky and Stewart [10]. Their approach uses a more abstract setting, and has lead to new mathematical questions about the dynamics of coupled cell systems in general. Viewing the motorneurons and CPG as a combined network with left–right $\mathbf{Z}_2$-symmetry, but with interior $\mathbf{D}_n$-symmetries in the motorneurons subnetworks, the authors show the existence of a periodic state called *synchro-traveling*. In such a state, cells in a subset oscillate periodically and in synchrony while cells in a disjoint subset oscillate in an approximate discrete traveling wave. A consequence of this approach is that both synchronous and peristaltic states have the same frequency. Moreover, the phase shifts of the peristaltic state vary along the array of motorneurons, as is the case of the actual system. Although the authors do not include a switching mechanism in the model, they suggest some ways to induce periodic transitions from one synchro-traveling state to a symmetric synchro-traveling wave. Another significant difference between their work and ours, is that in [10] the CPG plays an almost passive role in the generation of the motorneuron rhythms.

In this paper, we have adopted the fundamental assumption that the cells that model the array of motorneurons are coupled in some predetermined fashion. Since the experimental evidence that is available so far has not confirmed the existence of such connections, we would like to discuss, for completeness, some alternative methods of obtaining peristaltic and synchronous waves in uncoupled arrays of cells. We start by briefly reviewing related work by Thompson and Stent.

Thompson and Stent [29] present a mechanism to produce the two types of waves seen in the motorneuron networks. Their analysis is based, primarily, on timing the blending of the inhibitory postsynaptic potentials (IPSP) from the interneurons of the CPG, which keep the activity of the motorneurons below their action potential threshold. More precisely, by looking at the time lag between the arrival of the IPSPs to neighboring motorneurons along the array, they estimate the phase relations that an interneuron HN maintains relative to the overall beat cycle. This information is incorporated into a model which consists of a periodic function a_{ij} for the amplitude of the periodic inhibitory input from HN(i) to HE(j). Using the phase relations estimated experimentally in a_{ij} and obtaining an expression for the sum of the a_{ij}'s, they obtained relatively good agreement with the observed phase lags in the motorneuron array.

An alternative approach to the one proposed in [29] is to model the CPG and motorneuron array using a skew-product system of differential equations. Since the cells that model the motorneurons are assumed not to be coupled together, then the CPG-motorneurons system would consist of the CPG driving each motorneuron independently. Thus, for each motorneuron, the model would be written as a skew-product system of differential equations. However, the coupling between the various interneurons of the CPG and each motorneuron would be dependent on a delay argument modeling the time lag caused by the conduction time of the action potential in the axons. So the blending of the CPG output as well as the delays in conduction would be crucial to obtaining the peristaltic and synchronous waves. Modeling the different components of the system could be achieved using various types of well-known equations. For instance, the output of the CPG could be modeled using equations developed by Calabrese et al. [7,23] as is done in our numerical simulations, see Section 6, while the motorneuron dynamic would be described by a simple differential equation model for tonic firing. Now, such a model could only be analyzed using numerical simulations. It might be wise to consider simpler models, or toy models, to get insight into the dynamical behavior produced by variations of the blending and the delays in the input from the CPG to the motorneuron.

The dynamics of the motorneurons activity in the leech's heartbeat is an example of nontrivial periodic dynamics in a biological system. Experimental studies have significantly contributed to identifying the role of each interneuron in the CPG and their connections with the motorneurons. This paper, on the other hand, is one of the first attempts

at integrating the CPG and motorneurons dynamics into a single model, which can also account for a possible mechanism for periodic transitions between two motorneuron rhythms. It is our hope that this work will stimulate further research in related biological systems, and increase the interaction between experimentalists and applied mathematicians. In fact, also recently, symmetry methods have been attracting more interest in modeling biological systems. For instance, in modeling the behavior of CPG dynamics for quadrupedal locomotion [1,11], in modeling pattern formation in the primary visual cortex [4], and in networks of pulse coupled oscillators [3].

Acknowledgements

Informative discussions with Ronald Calabrese, Mike Field, and Marty Golubitsky are gratefully acknowledged. The research of PLB is supported by the Natural Sciences and Engineering Research Council of Canada in the form of a postdoctoral fellowship.

References

[1] P.-L. Buono, M. Golubitsky, Models of central pattern generators for quadruped locomotion. I. Primary gaits, J. Math. Biol. 42 (2001) 291–326.
[2] P.-L. Buono, M. Golubitsky, A. Palacios, Heteroclinic cycles in rings of coupled cell, Physica D 143 (2000) 74–108.
[3] P.C. Bressloff, S. Coombes, Symmetry and phase-locking in a ring of pulse-coupled oscillators with distributed delays, Physica D 126 (1999) 99–122.
[4] P.C. Bressloff, J.D. Cowan, M. Golubitsky, P.J. Thomas, M.C. Wiener, Geometric visual hallucinations, Euclidean symmetry, and the functional architecture of striate cortex, Philos. Trans. R. Soc. London B 356 (2001) 299–330.
[5] R. Calabrese, The neural control of alternate heartbeat coordination states in the leech, *Hirudo medicinalis*, J. Comp. Physiol. 122 (1977) 111–143.
[6] R. Calabrese, J. Feldman, Intrinsic membrane properties and synaptic mechanisms in motor rhythm generators, in: P. Stein, S. Grillner, A. Selverston, D. Stuart (Eds.), Neurons, Networks, and Motor Behavior, MIT Press, Cambridge, MA, 1997, pp. 119–130.
[7] R. Calabrese, F. Nadim, O. Olsen, Heartbeat control in the medicinal leech: a model system for understanding the origin, coordination, and modulation of rhythmic motor patterns, J. Neurobiol. 27 (1995) 390–402.
[8] A. Cohen, S. Rossignol, S. Grillner (Eds.), Neural Control of Rhythmic Movements in Vertebrates, Wiley, New York, 1988.
[9] I. Epstein, M. Golubitsky, Symmetric patterns in linear arrays of coupled cells, Chaos 3 (1) (1995) 1–5.
[10] M. Golubitsky, I.N. Stewart, Interior symmetries in coupled cell networks motivated by the leech heart, Preprint.
[11] M. Golubitsky, I.N. Stewart, P.-L. Buono, J.J. Collins, A modular network for legged locomotion, Physica D 115 (1998) 56–72.
[12] S. Gramoll, J. Schmidt, R. Calabrese, Switching in the activity state of an interneuron that controls coordination of the hearts in the medicinal leech (*Hirudo Medicinalis*), J. Exp. Biol. 186 (1994) 157–171.
[13] M. Golubitsky, I.N. Stewart, D.G. Schaeffer, Singularities and Groups in Bifurcation Theory, vol. II, Applied Mathematical Science, vol. 69, Springer, New York, 1988.
[14] S. Grillner, J. Buchanan, P. Wallen, L. Brodin, Neural control of locomotion in lower vertebrates, in: A.H. Cohen, S. Rossignol, S. Grillner (Eds.), Neural Control of Rhythmic Movements in Vertebrates, Wiley, New York, 1988, pp. 129–166.
[15] R.M. Harris-Warrick, E. Marder, Modulation of neural networks for behavior, Annu. Rev. Neurosci. 14 (1991) 39–57.
[16] A.L. Hodgkin, A.F. Huxley, A quantitative description of membrane current and its application to conduction and excitation in nerve, J. Physiol. London 117 (1952) 500–544.
[17] D. Jonhston, J. Magee, C. Colbert, B. Christie, Active properties of neuronal dendrites, Annu. Rev. Neurosci. 19 (1996) 165–186.
[18] C. Koch, Computation and the single neuron, Nature 385 (16) (1997) 207–210.
[19] J. Lu, S. Gramoll, J. Schmidt, R. Calabrese, Motor pattern switching in the heartbeat pattern generator of the medicinal leech: membrane properties and lack of synaptic interaction in switch interneurons, J. Comp. Physiol. A 184 (1999) 311–324.
[20] J.C. Magee, D. Johnston, A synaptically controlled associative signal for Hebbian plasticity in hippocampal neurons, Science 275 (1997) 209–213.
[21] H. Markram, J. Lubke, M. Frotscher, B. Sakmann, Regulation of synaptic efficacy by coincidence of postsynaptic APs and EPSPs, Science 275 (1997) 213–215.
[22] D.W. Morton, H.J. Chiel, The timing of activity in motor neurons that produce radula movements distinguishes ingestion from rejection in *Aplysia*, J. Comp. Physiol. A 173 (1993) 519–536.
[23] F. Nadim, O. Olsen, E. De Schutter, R. Calabrese, Modeling the leech heartbeat elemental oscillator. I. Interactions of intrinsic and synaptic currents, J. Comp. Neurosci. 2 (1995) 216–235.

[24] A. Pikovsky, M. Rosenblum, J. Kurths, Synchronization: A Universal Concept in Nonlinear Sciences, Cambridge University, New York, 2001.
[25] J. Schmidt, R. Calabrese, Evidence that acetylcholine is an inhibitory transmitter of heart interneurons in the leech, J. Exp. Biol. 171 (1992) 329–347.
[26] G. Stuart, B. Sakmann, Active propagation of somatic action potentials into neocortical pyramidal cell dendrites, Nature 367 (1994) 69–72.
[27] G. Stuart, N. Spruston, B. Sakmann, M. Hausser, Action potential initiation and backpropagation in neurons of the mammalian CNS, Trends Neurosci. 20 (1997) 125–131.
[28] W. Thompson, G. Stent, Neuronal control of heartbeat in the medicinal leech. I. Generation of the vascular constriction rhythm by heart motorneurons, J. Comp. Physiol. 111 (1976) 261–279.
[29] W. Thompson, G. Stent, Neuronal control of heartbeat in the medicinal leech. II. Intersegmental coordination of heart motor neuron activity by heart interneurons, J. Comp. Physiol. 111 (1976) 281–307.
[30] W. Thompson, G. Stent, Neuronal control of heartbeat in the medicinal leech. III. Synaptic relations of heart interneurons, J. Comp. Physiol. 111 (1976) 309–333.
[31] X. Wang, J. Rinzel, Alternating and synchronous rhythms in reciprocally inhibitory model neurons, Neural Comput. 4 (1992) 84–97.
[32] K. Westberg, A. Kolta, P. Clavelou, G. Sandstrom, J. Lund, Evidence for functional compartmentalization of trigeminal muscle spindle afferents during fictive mastication in the rabbit, J. Neurosci. 12 (2000) 1145–1154.